Chloride-supported Tungsten Alkyne Complexes. Synthesis, Electronic and Molecular Structures of $[W_2Cl_4(\mu\text{-}Cl)_2(\mu\text{-}C_2R_2)(thf)_2]$ (R = H or Me) and $[WCl_4(\eta\text{-}C_2Me_2)(thf)]$(thf = tetrahydrofuran) *

Simon G. Bott, David L. Clark, Malcolm L. H. Green and Philip Mountford
Inorganic Chemistry Laboratory, South Parks Road, Oxford OX1 3QR, UK

The complex $Na[W_2Cl_7(thf)_5]$ (thf = tetrahydrofuran) reacts with alkynes to afford the dimetallatetrahedrane complexes $[W_2Cl_4(\mu\text{-}Cl)_2(\mu\text{-}RC_2R')(thf)_2]$ (**1**, R = R' = Me; **4**, R = R' = H; **5**, R = R' = Et; **6**, R = H, R' = Ph) for which the X-ray crystal structures of **1** and **4** have been determined. In contrast, treatment of the related $[W_2Cl_7(thf)_2]^-$ ion with C_2Me_2 yields the η-bound alkyne complex $[NBu^n_4][W_2Cl_4(\mu\text{-}Cl)_3(\eta\text{-}C_2Me_2)_2]$ **7**. The μ-alkyne complex **1** reacts with further C_2Me_2 to give low yields of the mononuclear η-alkyne derivative $[WCl_4(\eta\text{-}C_2Me_2)(thf)]$ **2** which has been structurally characterised. Treatment of **2** with pyridine(py) affords the corresponding adduct $[WCl_4(\eta\text{-}C_2Me_2)(py)]$ **3**. Treatment of **1** with one or two equivalents of $[N(PPh_3)_2]Cl$ gives the mono- or di-anionic derivatives $[N(PPh_3)_2][W_2Cl_5(\mu\text{-}Cl)_2(\mu\text{-}C_2Me_2)(thf)]$ **8** or $[N(PPh_3)_2]_2[W_2Cl_6(\mu\text{-}Cl)_2(\mu\text{-}C_2Me_2)]$ **9** respectively. Extended Hückel molecular orbital calculations suggest that tight metal–μ-alkyne binding in the ditungsten complexes $[W_2Cl_4(\mu\text{-}Cl)_2(\mu\text{-}RC_2R')(thf)_2]$ suppresses a potential second-order Jahn–Teller distortion in these systems.

In recent years there has been considerable interest in binuclear μ-alkyne derivatives of the transition metals, and in compounds containing bridging hydrocarbyl ligands in general.[1] Bridging alkyne derivatives may be formed for many transition metals and with a wider range of supporting ligands (*e.g.*, carbonyl, cyclopentadienyl or alkoxide). The most widely studied class of dinuclear compounds is that which contains metals either in low formal oxidation states supported by π-acceptor ligands {*e.g.*, $[Mo_2(\eta\text{-}C_5H_5)_2(CO)_4]$[2] and $[Co_2(CO)_8]$[3]}, or in higher oxidation states supported by π-donor ligands {*e.g.*, $[M_2(OR)_6(py)_x]$ (M = Mo or W, py = pyridine)[4] and $[W_2Cl_2(NMe_2)_4]$[5]}. In contrast, there are only a few examples of reactions of halide-supported dimers with alkynes. Most notably, the ditantalum compound $[Ta_2Cl_4(\mu\text{-}Cl)_2(\mu\text{-tht})(tht)_2]$ (tht = tetrahydrothiophene) reacts with alkynes to give mono- or di-nuclear derivatives depending upon the particular alkyne used.[6–9]

The ditungsten species $Na[W_2Cl_7(thf)_5]$ (thf = tetrahydrofuran) reported recently[10] contains a bridged W≡W triple bond and is therefore related to the Ta=Ta double-bonded compound $[Ta_2Cl_4(\mu\text{-}Cl)_2(\mu\text{-tht})(tht)_2]$ described above, differing by one unit in its metal–metal bond order. We were interested to see if the ditungsten complex might serve as a suitable precursor to halide-supported ditungsten alkyne derivatives. Herein we describe a study of the reactions of $Na[W_2Cl_7(thf)_5]$ with alkynes, and the structures, reactivity and bonding of the products obtained. Part of this work has been communicated.[11]

Results and Discussion

Formation of μ- and η-Alkyne Complexes.—When a dilute thf solution of $Na[W_2Cl_7(thf)_5]$ was treated with an excess of but-2-yne, the colour of the solution changed from an initial emerald green to green-brown, and a light grey finely divided precipitate (NaCl) was observed. Removal of volatiles under reduced pressure followed by extraction of the residues with warm toluene-dichloromethane (3:1 v/v) and subsequent crystallisation at −80 °C gave green microcrystals of $[W_2Cl_4(\mu\text{-}Cl)_2(\mu\text{-}C_2Me_2)(thf)_2]$ **1** in *ca.* 40% yield. The identity of **1** was elucidated from elemental analysis, ^1H and ^{13}C NMR spectroscopy, and an X-ray crystal-structure determination. Analytical and spectroscopic data characterising **1** and the other new compounds described below are presented in Table 1, and their proposed structures are shown in Scheme 1. Single crystals of **1** suitable for an X-ray diffraction analysis were grown by slow cooling of a hot toluene solution. The molecular structure of **1** is shown in Fig. 1, bond lengths and angles are listed in Table 2 and fractional atomic coordinates are given in Table 3.

Each tungsten atom in **1** achieves a pseudo-octahedral co-ordination environment if the alkyne unit is considered to occupy a single co-ordination site and the metal-metal bond is ignored. Compound **1** is a perpendicular bridge alkyne complex and is isostructural with the ditantalum species $[Ta_2Cl_4(\mu\text{-}Cl)_2(\mu\text{-}C_2Bu^t_2)(thf)_2]$.[6] The apparently related dimolybdenum compound $[Mo_2Cl_4(\mu\text{-}Cl)_2(\mu\text{-}C_2Bu^t_2)(OPCl_3)_2]$ has been reported, but no structural details are available.[12] Compound **1** is also related to the alkoxide-supported derivatives $[M_2(OPr^i)_4(\mu\text{-}OPr^i)_2(\mu\text{-}C_2H_2)(py)_2]$ (M = Mo or W),[4] and to the dimethylamide-supported species $[W_2Cl_2(NMe_2)_2(\mu\text{-}Cl)(\mu\text{-}NMe_2)(\mu\text{-}C_2H_2)(PMe_3)_2]$[13] and $[W_2Cl_x(NMe_2)_{6-x}(\mu\text{-}RC_2R')(py)_2]$ (x = 2, 3 or 4).[5]

A potentially interesting feature of the structure of **1** is the slight asymmetry in the $W_2(\mu\text{-}C_2Me_2)$ unit. Defining the internal carbon atoms of the alkyne as C_{ac}, the projection of the C_{ac}–C_{ac} vector is twisted slightly with respect to the W_2 axis (Fig. 1). This is reflected in a significant difference (0.15 Å) between the W(1)–C(1) and W(1)–C(1B) bond lengths, which translates as a deviation of θ *ca.* 9° from the ideal perpendicular bridge geometry (θ = 0°).

Calhorda and Hoffmann[14] predicted a somewhat larger

* μ-Acetylene-$\kappa^2C^1:\kappa^2C^2$- and μ-but-2-yne-$\kappa^2C^1:\kappa^2C^2$-di-μ-chloro-bis[dichloro(tetrahydrofuran)tungsten] (*W–W*) and (but-2-ene-2,3-diyl)tetrachloro(tetrahydrofuran)tungsten.

Supplementary data available: see Instructions for Authors, *J. Chem. Soc., Dalton Trans.*, 1991, Issue 1, pp. xviii–xxii.

Table 1 Analytical and spectroscopic data

Complex	Colour	Analysis[a] (%) C	H	Cl	NMR data[b]
1	Green	18.6 (18.5)	3.1 (3.1)	27.6 (27.3)	^{1}H: 4.34 (s, 6 H, Me), 4.22 (m, 8 H, OCH_2CH$_2$), 1.97 (m, 8 H, OCH$_2$CH_2) ^{13}C: 234.8 (s, *C*Me), 74.5 [t, *J*(CH) 189, O*C*H$_2$*C*H$_2$], 25.3 [t, *J*(CH) 187, OCH$_2$*C*H$_2$], 23.9 [q, *J*(CH) 178, C*Me*]
2[c]	Green	20.4 (20.6)	2.9 (3.0)	30.5 (30.3)	^{1}H: 4.61 (br m and s, 10 H, Me and OCH_2CH$_2$), 2.16 (br m, 4 H, OCH$_2$CH_2) ^{13}C-{^{1}H}: 280.7 [*J*(CW) 26 (14% by area), *C*Me], 72.9 (O*C*H$_2$CH$_2$), 20.0 (OCH$_2$*C*H$_2$), 15.7 (C*Me*)
3[d]	Lime green	23.8 (23.6)	2.6 (2.9)	30.6 (30.9)	^{1}H: 9.56 [d, 2 H, *J*(H$_o$H$_m$), 5.0, *o*-NC$_5$H$_5$], 6.79 [t, 1 H, *J*(H$_p$H$_m$) 5.0, *p*-NC$_5$H$_5$], 6.56 [t, 2 H, *J*(H$_m$H$_{o/p}$) 5.0, *m*-NC$_5$H$_5$], 4.19 (s, 6 H, Me) ^{13}C-{^{1}H}: 283.9 (*C*Me), 151.7 (NC$_5$H$_5$), 139.2 (NC$_5$H$_5$), 124.3 (NC$_5$H$_5$), 29.9 (C*Me*)
4	Green	15.8 (16.0)	2.3 (2.4)	28.0 (28.3)	^{1}H: 11.93 [s, 2 H, *J*(HW) 5.6 (27% by area), C*H*], 4.21 (m, 8 H, OCH_2CH$_2$), 1.99 (m, 8 H, OCH$_2$CH_2) ^{13}C: 230.5 [d, *J*(CH) 223, *J*(CW) 26 (25.4% by area), *C*H], 72.9 [t, *J*(CH) 163, O*C*H$_2$CH$_2$], 24.9 [t, *J*(CH) 165, OCH$_2$*C*H$_2$]
5	Green	20.4 (20.8)	3.1 (3.3)	26.8 (26.4)	^{1}H: 4.94 [q, 4 H, *J*(HH) 7.3, CH_2Me], 4.19 (m, 8 H, OCH_2CH$_2$), 1.95 (m, 8 H, OCH$_2$CH_2), 1.29 [t, 6 H, *J*(HH) 7.3, CH$_2$*Me*] ^{13}C-{^{1}H}: 233.0 (*C*Et), 74.1 (O*C*H$_2$CH$_2$), 33.1 (*C*H$_2$Me), 25.0 (OCH$_2$*C*H$_2$), 13.3 (CH$_2$*Me*)
6[e]	Green	22.4 (22.4)	2.7 (2.6)	29.8 (30.1)	^{1}H: 12.62 [s, 2 H, *J*(HW) 5.6 (23% by area), C*H*], 7.54 [t, 2 H, *J*(H$_m$H$_{o/p}$) 17.9, *m*-C$_6$H$_5$], 6.62 [t, 1 H, *J*(H$_p$H$_m$) 17.9, *p*-C$_6$H$_5$], 6.39 [d, 2 H, *J*(H$_o$H$_m$) 7.9, *o*-C$_6$H$_5$], 4.23 (m, 8 H, OCH_2CH$_2$), 1.99 (m, 8 H, OCH$_2$CH_2) ^{13}C-{^{1}H}: 234.1 (*C*Ph), 228.1 [*J*(CW) 26 (25.7% by area), *C*H], 139.7 (*ipso*-C$_6$H$_5$), 132.7 (*o*- or *m*-C$_6$H$_5$), 131.9 (*p*-C$_6$H$_5$), 124.5 (*m*- or *o*-C$_6$H$_5$), 73.2 (OCH_2CH$_2$), 24.9 (OCH$_2$*C*H$_2$)
7[f]	Burgundy	29.1 (29.3)	5.9 (6.1)	25.1 (25.2)	^{1}H: 3.13 (m, 8 H, NCH$_2$), 3.08 (s, 12 H, C*Me*), 1.62 (m, 8 H, NCH$_2$CH_2), 1.44 (m, 8 H, CH_2Me), 1.02 [t, 12 H, *J*(HH) 7.8, CH$_2$*Me*] ^{13}C-{^{1}H}: 217.8 (*C*Me), 59.5 (NCH$_2$), 24.3 (NCH$_2$*C*H$_2$), 21.5 (C*Me*), 20.0 (*C*H$_2$Me), 13.7 (CH$_2$*Me*)
8[g]	Turquoise	41.0 (41.3)	3.4 (3.5)	19.8 (19.4)	^{1}H: 7.67 (m, 6 H, C$_6$H$_5$), 7.48 (m, 24 H, C$_6$H$_5$), 4.19 (m, 4 H, OCH_2CH$_2$), 3.70 (s, 6 H, Me), 1.88 (m, 4 H, OCH$_2$CH_2) ^{13}C-{^{1}H}: 223.9 [*J*(CW) 25 (26.3% by area), *C*Me], 133.5 (*p*-C$_6$H$_5$), 131.8 [d, *J*(CP) 6, *o*- or *m*-C$_6$H$_5$], 129.2 [d, *J*(CP) 7, *m*- or *o*-C$_6$H$_5$], 126.7 [d, *J*(CP) 108, *ipso*-C$_6$H$_5$], 73.1 (O*C*H$_2$CH$_2$), 24.8 (OCH$_2$*C*H$_2$), 22.3 (C*Me*)
9[h]	Turquoise	49.9 (51.2)	3.6 (3.7)	15.6 (15.9)	^{1}H: 7.66 (m, 12 H, C$_6$H$_5$), 7.48 (m, 48 H, C$_6$H$_5$), 3.45 (s, 6 H, Me) ^{13}C-{^{1}H}: 220.2 [*J*(CW) 23 (28.8% by area), *C*Me], 133.9 (*p*-C$_6$H$_5$), 132.3 [d, *J*(CP), 6, *o*- or *m*-C$_6$H$_5$], 129.7 [d, *J*(CP) 7, *m*- or *o*-C$_6$H$_5$], 127.1 [d, *J*(CP) 108, *ipso*-C$_6$H$_5$], 22.0 (C*Me*)

[a] Calculated values given in parentheses. [b] In [^{2}H$_2$]dichloromethane at 25 °C; data given as: chemical shift (δ), multiplicity (s = singlet, d = doublet, t = triplet, m = multiplet), coupling constant (in Hz), relative intensity and assignment. [c] ν(C≡C) (Nujol mull) at 1752m cm^{-1}. [d] N: 3.0 (3.1%); ν(C≡C) (Nujol mull) at 1749m cm^{-1}. [e] Analysis for [W$_2$Cl$_4$(μ-Cl)$_2$(μ-HC$_2$Ph)(thf)$_2$]·CH$_2$Cl$_2$. [f] N: 5.9 (6.1%); ν(C≡C) (Nujol mull) at 1753m cm^{-1}. [g] N: 1.0 (1.1%). [h] N: 1.4 (1.6%).

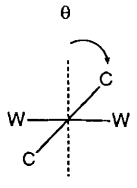

distortion of θ *ca.* 26° for the related model complex [W$_2$Cl$_6$(μ-NH$_2$)$_2$(μ-C$_2$H$_2$)]$^{2-}$ based on extended Hückel molecular orbital calculations. In compound **1**, however, the twist is much smaller and could be attributed to steric packing forces alone, although there appear to be no unusual intermolecular contacts (shortest intermolecular contact 2.674 Å, this being a H···H separation).

The ^{1}H and ^{13}C NMR spectra of **1** are consistent with the solid-state structure and show signals assignable to co-ordinated thf and C$_2$Me$_2$ ligands. The ^{13}C resonance for the internal carbon atoms (C$_{ac}$) of the μ-C$_2$Me$_2$ ligand is located at δ 234.8 ppm and is the largest yet reported for a M$_2$(μ-alkyne) complex.

A second, minor diamagnetic product from the reaction of Na[W$_2$Cl$_7$(thf)$_5$] with C$_2$Me$_2$ was the mononuclear η-alkyne derivative, [WCl$_4$(η-C$_2$Me$_2$)(thf)] **2**. The corresponding pyridine adduct [WCl$_4$(η-C$_2$Me$_2$)(py)] **3** could be isolated as pale green microcrystals by adding pyridine to **2** in CH$_2$Cl$_2$. Compound **2** (and subsequently **3**) can be prepared independently by a method analogous to that reported by Schrock and co-workers[15] for some other [WCl$_4$(η-C$_2$R$_2$)L] species. Thus treatment of WCl$_4$ with an excess of C$_2$Me$_2$ in diethyl ether for several days, followed by crystallisation from thf, afforded **2** in *ca.* 60% yield.

Single crystals of **2** suitable for an X-ray structure determination were obtained by slow cooling of a thf solution. The molecular structure of **2** is shown in Fig. 2, selected bond lengths and angles are listed in Table 4 and fractional atomic coordinates are given in Table 5. The molecular structure of **2** may be described as a pseudo-octahedral tungsten complex with four chloride ligands in the equatorial plane and mutually *trans* thf and η-C$_2$Me$_2$ ligands. The C(6)–C(7) (C$_{ac}$–C$_{ac}$) vector is staggered with respect to the WCl$_4$(thf) fragment and so its projection onto the WCl$_4$ plane bisects two of the Cl–W–Cl angles. The W atom lies approximately 0.29 Å out of the least-squares plane of the four chloride ligands. The C$_{ac}$–C$_{ac}$ distance in **2** [1.300(9) Å] is notably shorter than in the dinuclear species **1** [C$_{ac}$–C$_{ac}$ 1.39(1) Å] consistent with a more substantial reduction of the alkyne fragment in the latter complex.

The IR and NMR spectroscopic data and the values of M–C$_{ac}$

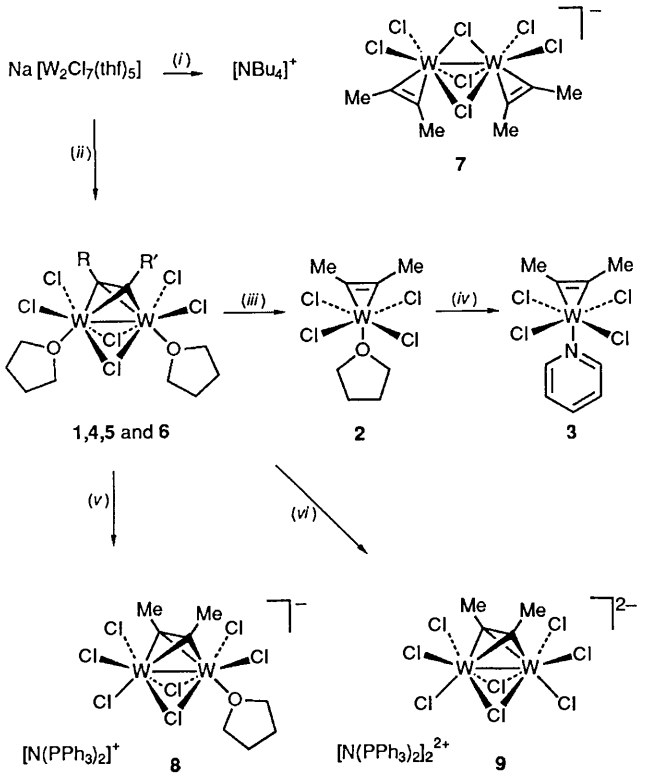

Scheme 1 (*i*) $[NBu^n_4]Cl$ (1 equiv.), CH_2Cl_2, 16 h, r.t., then excess of C_2Me_2, 3 h, r.t. (27%); (*ii*) excess of RC_2R', thf, r.t., where R = R′ = Me (**1**, 40%), R = R′ = H (**4**, 30%), R = R′ = Et (**5**, 25%), R = H, R′ = Ph (**6**, 35%); (*iii*) for R = R′ = Me (**1**), excess of C_2Me_2, CH_2Cl_2, r.t. (11% isolated yield, 20% by ^1H NMR); (*iv*) excess of pyridine, CH_2Cl_2, 8 h, r.t (*ca.* 100%); (*v*) for R = R′ = Me (**1**), $[N(PPh_3)_2]Cl$ (1 equiv.), CH_2Cl_2, 3 h, r.t. (*ca.* 100%); (*vi*) for R = R′ = Me (**1**), $[N(PPh_3)_2]Cl$ (2 equiv.), CH_2Cl_2, 3 h, r.t. (*ca.* 100%)

[average 2.002(8) Å] and C_{ac}–C_{ac} [1.300(9) Å] for **2** are similar to those observed for other pseudo-octahedral d^2 η-alkyne complexes.[7,16,17] The chemical shifts for the acetylenic carbon atoms in the tetrachloro complexes **2** and **3** (280.7 and 283.9 ppm respectively), and those reported for related examples, are the furthest downfield known for η^2-alkyne compounds. Much of this chemical shift can be ascribed to the inductive effects of a near-total chloride ligand environment. The chemical shifts for the alkyne carbon atoms in analogous methyl and *tert*-butoxide complexes are substantially lower {*e.g.*, δ(C_{ac}) in $[W(OBu^t)_4(\eta\text{-}C_2Ph_2)]$ is 202.0 ppm[15]}. It is likely, however, that for the alkoxide complexes significant $p_\pi \rightarrow d_\pi$ donation from the oxygen 2p orbitals must also be taken into account in addition to any inductive effects.

For η^2-C_2R_2 complexes described here, the ^{13}C NMR data suggest that the alkyne ligand acts as a formal four-electron donor under the Templeton notation.[18] That is to say, both sets of alkyne π-bonding electrons appear to be involved substantially in metal-alkyne bonding, and the alkyne contributes four electrons to the formal electron count of the metal atom. Together with the short W–C_{ac} bond lengths and the C_{ac}–C_{ac} separation of 1.300(9) Å (close to that expected for a C=C double bond) this suggests a formal oxidation state of VI for **2** and **3**. These conclusions are consistent with Cotton's description of this type of complex as metallacyclopropene-like rather than as a simple alkyne complex.[17]

Treatment of $Na[W_2Cl_7(thf)_5]$ with C_2H_2, HC_2Ph or C_2Et_2 also affords μ-alkyne derivatives. Thus the compounds $[W_2Cl_4(\mu\text{-}Cl)_2(\mu\text{-}RC_2R')(thf)_2]$ (**4**, R = R′ = H; **5**, R = R′ = Et; **6**, R = H, R′ = Ph) were prepared in *ca.* 25–35% yield. Compounds **4**–**6** all have ^1H and ^{13}C NMR spectra (Table 1)

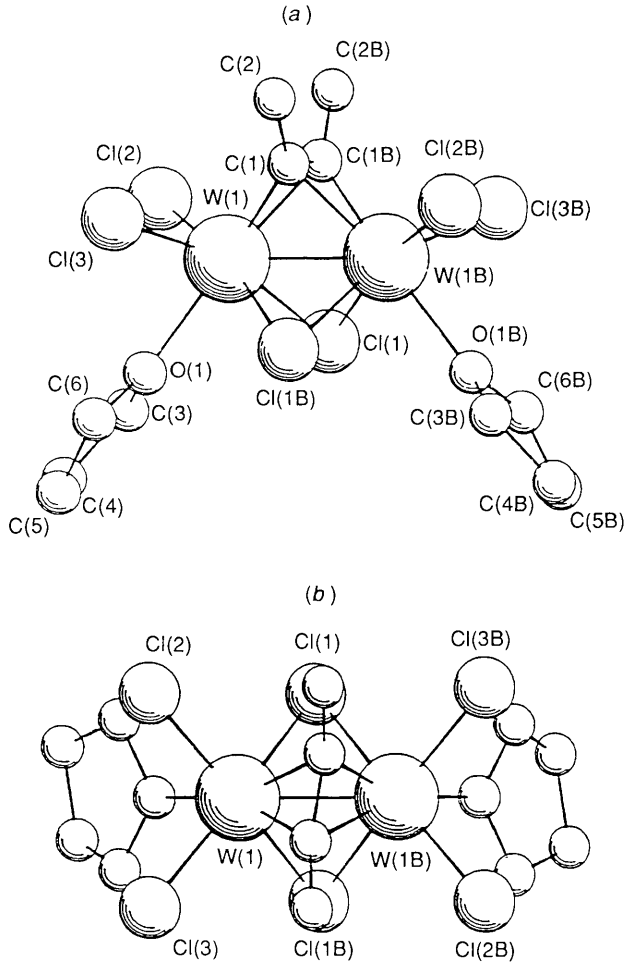

Fig. 1 Two views of $[W_2Cl_4(\mu\text{-}Cl)_2(\mu\text{-}C_2Me_2)(thf)_2]$ **1**. (*a*) Viewed nearly perpendicular to the W–W bond. (*b*) Viewed along the crystallographic two-fold rotation axis. Hydrogen atoms have been omitted for clarity. Atoms designated 'B' are related to their counterparts by a crystallographic two-fold axis

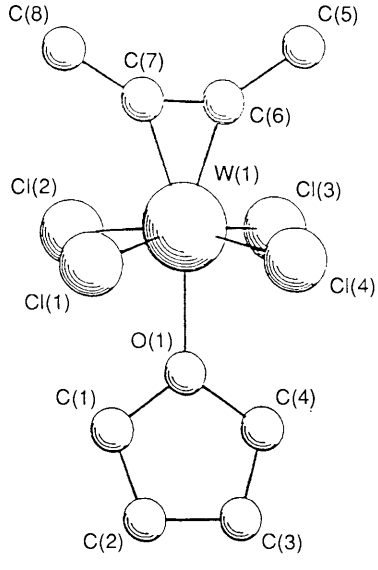

Fig. 2 Molecular structure of $[WCl_4(\eta\text{-}C_2Me_2)(thf)]$ **2**. Hydrogen atoms omitted for clarity

consistent with the preservation of structures analogous to that of **1**, exhibiting resonances assignable to coordinated thf and RC_2R' ligands. The ^{13}C chemical shifts for the acetylenic carbons are all in the range δ 210–230 ppm. Where ^{13}C–^{183}W

Table 2 Bond lengths (Å) and angles (°) for $[W_2Cl_4(\mu\text{-}Cl)_2(\mu\text{-}C_2Me_2)(thf)_2]$ **1** with estimated standard deviations in parentheses

W(1)–W(1B)	2.5863(6)	W(1)–Cl(1)	2.485(2)
W(1)–Cl(1B)	2.486(2)	W(1)–Cl(2)	2.331(2)
W(1)–Cl(3)	2.348(2)	W(1)–O(1)	2.224(7)
W(1)–C(1)	2.01(1)	W(1)–C(1B)	2.16(1)
O(1)–C(3)	1.49(1)	O(1)–C(6)	1.44(1)
C(1)–C(1B)	1.39(2)	C(1)–C(2)	1.50(1)
C(3)–C(4)	1.46(2)	C(4)–C(5)	1.49(2)
C(5)–C(6)	1.42(2)		
Cl(1)–W(1)–W(1B)	58.67(5)	Cl(1)–W(1)–W(1B)	58.62(5)
Cl(1)–W(1)–Cl(1B)	82.34(9)	Cl(2)–W(1)–W(1B)	126.65(7)
Cl(2)–W(1)–Cl(1)	92.51(8)	Cl(2)–W(1)–Cl(1B)	168.73(9)
Cl(3)–W(1)–W(1)	127.89(7)	Cl(3)–W(1)–Cl(1B)	164.0(1)
Cl(3)–W(1)–Cl(1)	89.80(9)	Cl(3)–W(1)–Cl(2)	92.65(9)
O(1)–W(1)–W(1B)	126.9(2)	O(1)–W(1)–Cl(1)	82.8(2)
O(1)–W(1)–Cl(1B)	83.1(2)	O(1)–W(1)–Cl(2)	86.3(2)
O(1)–W(1)–Cl(3)	82.4(2)	C(1)–W(1)–W(1B)	54.4(3)
C(1)–W(1)–Cl(1)	108.9(4)	C(1)–W(1)–Cl(1B)	82.7(3)
C(1)–W(1)–Cl(2)	108.5(3)	C(1)–W(1)–Cl(3)	83.8(4)
C(1)–W(1)–O(1)	160.3(4)	C(1)–W(1)–W(1B)	49.0(3)
C(1)–W(1)–Cl(1)	79.8(3)	C(1)–W(1)–Cl(1B)	103.8(3)
C(1)–W(1)–Cl(2)	85.0(3)	C(1)–W(1)–Cl(3)	115.8(3)
C(1)–W(1)–O(1)	160.1(3)	C(1)–W(1)–C(1B)	38.8(6)
W(1)–Cl(1)–W(1B)	62.70(5)	C(3)–O(1)–W(1)	124.2(6)
C(6)–O(1)–W(1)	127.6(7)	C(6)–O(1)–C(3)	108.0(9)
W(1)–C(1)–W(1B)	76.6(4)	C(1)–C(1B)–W(1)	76.7(6)
C(1)–C(1B)–W(1B)	64.6(7)	C(2)–C(1)–W(1)	139.7(10)
C(2)–C(1)–W(1B)	134.7(8)	C(2)–C(1)–C(1B)	134.5(8)
C(4)–C(3)–O(1)	107.1(11)	C(5)–C(4)–C(3)	105.8(11)
C(6)–C(5)–C(4)	108.3(12)	C(5)–C(6)–O(1)	107.8(12)

Table 3 Fractional atomic coordinates (× 10^4) for complex **1**

Atom	*X/a*	*Y/b*	*Z/c*
W(1)	1280.4(3)	1430.2(4)	3055.5(2)
Cl(1)	−504(2)	−283(3)	3570(2)
Cl(2)	2146(3)	2526(4)	4737(2)
Cl(3)	3240(3)	2300(4)	2550(2)
O(1)	2599(6)	−823(10)	3635(5)
C(1)	336(13)	3305(13)	2106(7)
C(2)	661(14)	4641(19)	1403(10)
C(3)	2764(15)	−1611(18)	4677(11)
C(4)	3804(16)	−2942(19)	4793(12)
C(5)	4052(17)	−3133(21)	3743(12)
C(6)	3528(15)	−1673(18)	3142(12)

coupling is observed, the ^{183}W satellites have the proper intensity for coupling to two equivalent tungsten atoms.

In contrast, no corresponding μ-alkyne derivatives could be obtained from treating $Na[W_2Cl_7(thf)_5]$ with C_2Ph_2, $C_2(SiMe_3)_2$ or $C_2(CF_3)_2$. With $C_2(SiMe_3)_2$ and $C_2(CF_3)_2$ no visible reaction occurred even at elevated temperatures over several days, whereas $Na[W_2Cl_7(thf)_5]$ reacted slowly with C_2Ph_2 to give a dark red-brown solution from which no discrete product could be isolated or identified.

In order to understand better the importance of the apparent 'twist' in the μ-alkyne ligand of **1**, we determined the X-ray crystal structure of the ethyne homologue, $[W_2Cl_4(\mu\text{-}Cl)_2(\mu\text{-}C_2H_2)(thf)_2]$ **4**. Thin, needle-like crystals of **4** were obtained by slow evaporation of a dichloromethane solution. The molecular structure of **4** is shown in Fig. 3, selected bond lengths and angles are listed in Table 6 and fractional atomic coordinates are given in Table 7.

As expected, the molecular structures of **1** and **4** are largely identical. Two notable differences are an increase of 0.037 Å in the W(1)–W(1B) bond length from 2.5863(6) Å in **1** to 2.6233(9) Å in **4**, and an increase in the C(1)–C(1B) bond length from 1.39(2) Å in **1** to 1.42(3) Å in **4**. Only the difference in metal–metal bond length is significant within the estimated errors

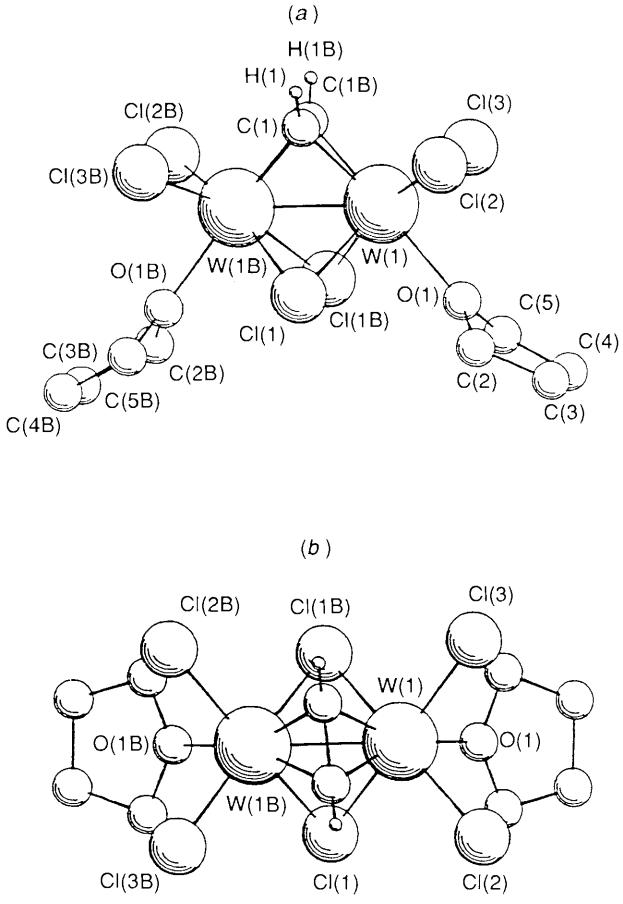

Fig. 3 Two views of $[W_2Cl_4(\mu\text{-}Cl)_2(\mu\text{-}C_2H_2)(thf)_2]$ **4**. (*a*) Viewed nearly perpendicular to the W–W bond. (*b*) Viewed along the crystallographic two-fold rotation axis. Methylene hydrogen atoms have been omitted for clarity. Atoms designated 'B' are related to their counterparts by a crystallographic two-fold axis

associated with these distances, but may indicate a slightly stronger interaction between the C_2H_2 and $W_2Cl_4(\mu\text{-}Cl)_2(thf)_2$ fragments. The principal purpose for determining the molecular structure of **4** was to investigate the apparent 'twist' of the μ-alkyne ligand in the absence of possible steric interactions such as those which may arise from the methyl groups of the but-2-yne ligand in **1**. In compound **4**, any differences in W–C_{ac} bond lengths are now no longer significant within their estimated errors, and any 'twist' present in this species is less than θ *ca.* 5°. We shall explore the reasons for the lack of the potential 'twist' in the complexes $[W_2Cl_4(\mu\text{-}Cl)_2(\mu\text{-}C_2R_2)(thf)_2]$ (R = H or Me) later.

A comparison of important structural data for **1** and **4** may be made with those of related Group 5 and 6 complexes with perpendicular bridge alkynes. The C_{ac}–C_{ac} bond lengths in the chloride-supported derivatives **1** [1.39(2) Å] and **4** [1.42(3) Å] are amongst the longest known for μ-alkyne complexes. They are similar to those found in the related alkoxide- and dimethylamide-supported complexes $[M_2(OPr^i)_4(\mu\text{-}OPr^i)_2(\mu\text{-}C_2H_2)(py)_2]$ (M = Mo or W) and $[W_2Cl_2(NMe_2)_2(\mu\text{-}NMe_2)_2(\mu\text{-}C_2H_2)(py)_2]$ [1.368(6), 1.39(2), and 1.375(11) Å respectively[5,19]]. The W–W bond lengths in **1** and **4** are markedly lengthened from that of the starting material[10] $Na[W_2Cl_7(thf)_5]$ [W≡W 2.4028(15) Å], and are consistent with a substantial delocalisation of metal–metal bonding electrons away from the dimetal centre towards the alkyne. This lengthening of the metal–metal bond on co-ordination of a μ-alkyne ligand is a notable difference from the ditantalum analogue $[Ta_2Cl_4(\mu\text{-}Cl)_2(\mu\text{-}C_2Bu^t_2)(thf)_2]$ in which the Ta=Ta bond length is in fact slightly *shorter* than that of the doubly bonded precursor $[Ta_2Cl_4(\mu\text{-}Cl)_2(\mu\text{-}tht)(tht)_2]$.[20] Moreover,

Table 4 Bond lengths (Å) and angles (°) for $[WCl_4(\eta\text{-}C_2Me_2)(thf)]$ **2** with estimated standard deviations in parentheses

W(1)–Cl(1)	2.357(2)	W(1)–Cl(2)	2.352(1)
W(1)–Cl(3)	2.350(2)	W(1)–Cl(4)	2.343(2)
W(1)–O(1)	2.242(4)	W(1)–C(6)	2.001(6)
W(1)–C(7)	2.004(6)	O(1)–C(1)	1.448(8)
O(1)–C(4)	1.458(8)	C(1)–C(2)	1.51(1)
C(2)–C(3)	1.51(1)	C(3)–C(4)	1.48(1)
C(5)–C(6)	1.48(1)	C(6)–C(7)	1.300(9)
C(7)–C(8)	1.465(9)		
Cl(2)–W(1)–Cl(1)	89.67(6)	Cl(3)–W(1)–Cl(1)	165.26(6)
Cl(3)–W(1)–Cl(2)	87.15(6)	Cl(4)–W(1)–Cl(1)	87.70(6)
Cl(4)–W(1)–Cl(2)	165.53(6)	Cl(4)–W(1)–Cl(3)	91.80(7)
O(1)–W(1)–Cl(1)	82.3(1)	O(1)–W(1)–Cl(2)	83.3(1)
O(1)–W(1)–Cl(3)	83.1(1)	O(1)–W(1)–Cl(4)	82.2(1)
C(6)–W(1)–Cl(1)	109.9(2)	C(6)–W(1)–Cl(2)	110.9(2)
C(6)–W(1)–Cl(3)	84.6(2)	C(6)–W(1)–Cl(4)	83.4(2)
C(6)–W(1)–O(1)	160.7(2)	C(7)–W(1)–Cl(1)	83.7(2)
C(7)–W(1)–Cl(2)	84.3(2)	C(7)–W(1)–Cl(3)	110.2(2)
C(7)–W(1)–Cl(4)	109.5(2)	C(7)–W(1)–O(1)	161.4(2)
C(7)–W(1)–C(6)	37.9(3)	C(1)–O(1)–W(1)	126.3(4)
C(4)–O(1)–W(1)	126.5(4)	C(4)–O(1)–C(1)	106.4(5)
C(2)–C(1)–O(1)	104.2(6)	C(3)–C(2)–C(1)	104.9(6)
C(4)–C(3)–C(2)	106.5(6)	C(3)–C(4)–O(1)	106.2(6)
C(5)–C(6)–W(1)	142.3(5)	C(7)–C(6)–W(1)	71.2(4)
C(7)–C(6)–C(5)	146.5(7)	C(6)–C(7)–W(1)	70.9(4)
C(8)–C(7)–W(1)	142.2(5)	C(8)–C(7)–C(6)	146.8(6)

Table 5 Fractional atomic coordinates ($\times 10^4$) for $[WCl_4(\eta\text{-}C_2Me_2)(thf)]$ **2**

Atom	*X/a*	*Y/b*	*Z/c*
W(1)	3 083.8(3)	8 330.3(3)	8 632.16(9)
Cl(1)	3 206(2)	6 922(2)	9 532.2(7)
Cl(2)	5 771(2)	9 751(2)	8 890.1(7)
Cl(3)	2 764(2)	10 412(2)	7 864.1(7)
Cl(4)	151(2)	7 531(3)	8 509.0(8)
O(1)	2 070(6)	10 745(7)	9 100(2)
C(1)	2 848(10)	11 538(11)	9 626(3)
C(2)	1 350(11)	12 406(12)	9 890(3)
C(3)	41(10)	12 861(11)	9 397(3)
C(4)	683(12)	12 009(12)	8 891(4)
C(5)	2 456(11)	5 710(13)	7 489(3)
C(6)	3 284(8)	6 382(9)	8 038(3)
C(7)	4 510(8)	6 130(9)	8 445(3)
C(8)	6 000(9)	5 004(11)	8 664(4)

Table 6 Bond lengths (Å) and angles (°) for $[W_2Cl_4(\mu\text{-}Cl)_2(\mu\text{-}C_2H_2)(thf)_2]$ **4** with estimated standard deviations in parentheses

W(1)–W(1B)	2.6233(9)	W(1)–Cl(1)	2.486(3)
W(1)–Cl(1B)	2.486(3)	W(1)–Cl(2)	2.344(4)
W(1)–Cl(3)	2.343(3)	W(1)–O(1)	2.228(9)
W(1)–C(1)	2.04(1)	W(1)–C(1B)	2.09(1)
O(1)–C(2)	1.44(2)	O(1)–C(5)	1.48(2)
C(1)–C(1B)	1.42(3)	C(2)–C(3)	1.47(2)
C(3)–C(4)	1.52(3)	C(4)–C(5)	1.51(2)
Cl(1)–W(1)–W(1B)	58.15(7)	Cl(1B)–W(1)–W(1B)	58.16(7)
Cl(1)–W(1)–Cl(1B)	78.1(1)	Cl(2)–W(1)–W(1B)	126.73(9)
Cl(2)–W(1)–Cl(1)	93.0(1)	Cl(2)–W(1)–Cl(1B)	165.1(2)
Cl(3)–W(1)–W(1B)	126.0(1)	Cl(3)–W(1)–Cl(1)	165.1(2)
Cl(3)–W(1)–Cl(1B)	92.3(1)	Cl(3)–W(1)–Cl(2)	93.8(1)
O(1)–W(1)–W(1B)	128.9(3)	O(1)–W(1)–Cl(1)	82.8(3)
O(1)–W(1)–Cl(1B)	84.4(3)	O(1)–W(1)–Cl(2)	82.7(3)
O(1)–W(1)–Cl(3)	85.9(3)	C(1)–W(1)–W(1B)	51.6(4)
C(1)–W(1)–Cl(1)	81.6(4)	C(1)–W(1)–Cl(1B)	106.9(4)
C(1)–W(1)–Cl(2)	83.2(4)	C(1)–W(1)–Cl(3)	112.4(4)
C(1)–W(1)–O(1)	158.3(5)	C(1)–W(1)–W(1B)	49.6(4)
C(1)–W(1)–Cl(1)	105.0(4)	C(1)–W(1)–Cl(1B)	80.5(4)
C(1)–W(1)–Cl(2)	113.6(5)	C(1)–W(1)–Cl(3)	84.3(4)
C(1)–W(1)–O(1)	161.0(5)	C(1)–W(4)–C(1B)	40.1(8)
W(1)–Cl(1)–W(1B)	63.69(8)	C(2)–O(1)–W(1)	126.0(8)
C(5)–O(1)–W(1)	124.5(10)	C(5)–O(1)–C(2)	108.7(13)
W(1)–C(1)–W(1B)	78.8(5)	C(1)–C(1B)–W(1)	72.2(8)
C(1)–C(1B)–W(1B)	67.7(8)	C(3)–C(2)–C(1)	106.3(12)
C(4)–C(3)–C(2)	105.4(14)	C(5)–C(4)–C(3)	107.6(15)

Table 7 Fractional atomic coordinates ($\times 10^4$) for $[W_2Cl_4(\mu\text{-}Cl)_2(\mu\text{-}C_2H_2)(thf)_2]$ **4**

Atom	*X/a*	*Y/b*	*Z/c*
W(1)	4379.8(2)	2283.1(9)	2422.6(4)
Cl(1)	4767(2)	301(5)	1171(2)
Cl(2)	3463(2)	3397(7)	896(3)
Cl(3)	3986(2)	3398(7)	3802(3)
O(1)	3711(5)	−142(15)	2299(8)
C(1)	4873(7)	4285(21)	1898(13)
C(2)	3348(8)	−1166(29)	1282(14)
C(3)	2796(9)	−2081(26)	1492(17)
C(4)	2987(11)	−2056(27)	2777(17)
C(5)	3663(9)	−1158(36)	3288(14)

the C_{ac}–C_{ac} distance in the ditantalum species [C_{ac}–C_{ac} 1.321(21) Å] may suggest diminished alkyne reduction in this complex relative to that in **1** and **4**. The W–W bond lengths of **1** and **4** are similar to those of the alkoxide and dimethylamide complexes discussed above, and the W–C_{ac} distances in **1** and **4** are much shorter than the corresponding average Ta–C_{ac} distance [2.32(11) Å] in the ditantalum analogue.[6]

The structural differences between the ditungsten and ditantalum $[M_2Cl_4(\mu\text{-}Cl)_2(\mu\text{-}C_2R_2)(thf)_2]$ systems may be rationalised in terms of extended Hückel calculations reported by Hoffmann and co-workers[21] for the model complexes $[M_2Cl_4(\mu\text{-}Cl)_2(\mu\text{-}C_2H_2)H_2]^{2-}$ where $(\pi)^2(\sigma)^2$ and $(\pi)^2(\sigma)^2(\pi^*)^2$ descriptions of the metal–metal bond were found for M = Ta and Mo respectively. Since the M–M π^* level also contains significant C_{ac}–C_{ac} antibonding and M–C_{ac} bonding character, the shorter M–C_{ac} and longer M–M and C_{ac}–C_{ac} distances in the Group 16 complexes are readily accounted for. The ditungsten and ditantalum dimers $[M_2Cl_4(\mu\text{-}Cl)_2(\mu\text{-}C_2R_2)(thf)_2]$ are therefore related in the same way as the dicobalt and diiron hexacarbonyl derivatives $[M_2(CO)_6(\mu\text{-}C_2Bu^t_2)]$.[22]

It has been noted previously that for alkynes bridging a dimetal centre very few have C_{ac}–C_{ac} bond lengths approaching those found in the alkoxide series $[M_2(OR)_6(\mu\text{-}C_2R'_2)(py)_x]$. This has been attributed to enhanced π back-bonding (and therefore enhanced alkyne reduction) in these systems on the basis of computational results.[23] Most of the other perpendicular bridge alkyne complexes involve middle to late transition metals in low oxidation states, with partial or total carbonyl (π-acceptor) ligand environments with the consequence that the metal d block of the alkoxide (π-donor) complexes is much higher in energy relative to most of the other $M_2(\mu\text{-alkyne})$ species and so a better energy match is made between the filled metal d orbitals and the empty π^* sets of the alkyne. Therefore, while π donation of electrons from the C_2R_2 ligand to the dimetal centre in alkoxide-supported $M_2(\mu\text{-}C_2R_2)$ complexes appears to be very similar to that of the cyclopentadienyl- and carbonyl-supported species, π donation of electron density from M_2 to C_2R_2 is larger.[21,23]

The structures of **1** and **4** suggest that the degree of alkyne reduction in the chloride-supported alkyne complexes is more like that found with good π-donor ligands than with good π-acceptor ligands. The relatively large downfield shifts of the C_{ac} atoms in the chloride-supported derivatives reported here compared to those for the related alkoxide-supported analogues are, however, consistent with the qualitative expectation of a greater degree of π donation from alkoxide ligands as compared to chloride ligands, and with molecular orbital calculations which have shown that back donation from M_2 to $\mu\text{-}C_2R_2$ in the

alkoxide series $[M_2(OR')_6(\mu\text{-}C_2R_2)(py)_x]$ is diminished on neglecting π donation from the alkoxide ligands.[23]

While this work was in progress, the sodium-free ditungsten anion $[W_2Cl_7(thf)_2]^-$, prepared *via* simple metathesis with tetraphenylphosphonium chloride, was reported [equation (1)].[24]

$$Na[W_2Cl_7(thf)_5] + [PPh_4]Cl \longrightarrow [PPh_4][W_2Cl_7(thf)_2] + NaCl \quad (1)$$

This metathesis reaction is related to the reaction that occurs between $Na[W_2Cl_7(thf)_5]$ and RC_2R' [equation (2)].

$$Na[W_2Cl_7(thf)_5] + RC_2R' \longrightarrow [W_2Cl_4(\mu\text{-}Cl)_2(\mu\text{-}RC_2R')(thf)_2] + NaCl \quad (2)$$

Since one possible 'driving force' in the reaction of $Na[W_2Cl_7(thf)_5]$ with alkynes is the formation of NaCl (*i.e.*, 'salt elimination'), it was of interest to see if μ-alkyne derivatives could be obtained from the reaction of the sodium-free complex $[W_2Cl_7(thf)_2]^-$ with, for example, C_2Me_2.

The green ditungsten anion $[W_2Cl_7(thf)_2]^-$ was prepared *in situ* by the addition of one equivalent of $[NBu^n_4]Cl$ to a dichloromethane solution of $Na[W_2Cl_7(thf)_5]$. Subsequent filtration to remove precipitated NaCl and addition of C_2Me_2 (4–5 equivalents) resulted in a colour change from green to red-brown. Layering of the dichloromethane solution with toluene afforded maroon microcrystals of $[NBu^n_4][W_2Cl_4(\mu\text{-}Cl)_3(\eta\text{-}C_2Me_2)_2]$ **7** (Scheme 1) which were characterised by elemental analysis, ^1H and ^{13}C NMR spectroscopy, and IR spectroscopy.

The $^{13}C\text{-}\{^1H\}$ NMR spectrum of **7** showed a singlet at 217.8 ppm assigned as the C_{ac} resonance of the C_2Me_2 ligand. An absorption at 1753 cm^{-1} in its IR spectrum (Nujol, CsI) was assigned as the ν(C≡C) stretch of an η^2-bound alkyne ligand. It is notable that in the μ-alkyne derivatives **1**, **4**, **5** and **6** that no ν(C≡C) modes were observed, whereas for the η^2-C_2Me_2 ligand in the mononuclear species **2** and **3**, bands at 1752 and 1749 cm^{-1} respectively were readily discernible. On the basis of these data we propose that **7** has the structure shown in Scheme 1, in which simple substitution of co-ordinated thf by C_2Me_2 has occurred.

It is not clear from the NMR and IR data alone what effect the terminal η-C_2Me_2 ligands have on the metal–metal bonding interactions, and therefore the formal metal-metal bond order, in this anion. Templeton and Ward[18] have established an empirical correlation of the ^{13}C chemical shift of the acetylenic carbons of η-bound alkynes with the number of electrons formally donated to the metal centre. The observed chemical shift of 217.8 ppm for the internal C_{ac} atoms in **7** is certainly consistent with the η-C_2Me_2 moiety acting as a four-electron donor based on their criteria. However, their correlation was established for mononuclear η-alkyne species with ancilliary ligands such as cyclopentadienyl, carbonyl, thiolate, *etc.*, and it is not clear how appropriate it is to use this correlation between δ ($^{13}C_{ac}$) and the number of electrons formally donated in the case of this dinuclear complex. It has already been observed that partial or total halide ligand environments can cause large downfield shifts of the $^{13}C_{ac}$ resonance. If the η-C_2Me_2 ligand in **7** does act as a four-electron donor, then simple electron counting procedures must require a W–W single bond. Similarly, if the W–η-C_2Me_2 bonding is predominantly metallacyclopropene in nature, then this amounts to an increase in formal oxidation state of W from +3 to +5, and again a W–W single bond is required. Only if the C_2Me_2 ligand acts as a simple two-electron donor (*i.e.*, in the same way as thf) is a formal W≡W triple bond possible.

Reaction Chemistry of $[W_2Cl_4(\mu\text{-}Cl)_2(\mu\text{-}C_2Me_2)(thf)_2]$.—Some perpendicular bridge alkyne compounds react with further equivalents of alkyne to give dinuclear products containing two or more coupled alkyne units.[2–4] However, when $[W_2Cl_4(\mu\text{-}Cl)_2(\mu\text{-}C_2Me_2)(thf)_2]$ **1** was treated with further but-2-yne a red-brown solution was obtained which was shown by ^1H NMR spectroscopy to contain hexamethylbenzene and $[WCl_4(\eta\text{-}C_2Me_2)(thf)]$ **2** as the only diamagnetic products. No other products could be isolated from the reaction mixture. When the reaction was monitored by ^1H NMR spectroscopy, it was found that **1** disappeared rapidly and that no further formation of **2** was observed after 20 min. However, formation of C_6Me_6 was not complete until 2–3 d later. The yields (by ^1H NMR spectroscopy) of **2** and C_6Me_6 were 20 and 35% respectively. A study of the reaction of **1** with C_2H_2 showed the formation of traces of **2** and benzene (80% yield based on **1**). A black insoluble precipitate was subsequently identified as a mixture of *cis*- and *trans*-polyacetylene by IR spectroscopy.

It is clear that in these reactions most of the tungsten-containing product was not observed and that the inorganic products identified account for only a small fraction of the ditungsten starting material. The formation of **2** and C_6Me_6 from the reaction of **1** with C_2Me_2 accounts for their occurrence in the preparation of **1** from $Na[W_2Cl_7(thf)_5]$ and C_2Me_2. The mononuclear compound $[WCl_4(\eta\text{-}C_2Me_2)(thf)]$ **2** does not react with further C_2Me_2. The species responsible for the formation of the cyclotrimerisation products is not known, but it is likely that this reaction involves low-valent co-ordinatively unsaturated mononuclear fragments arising from cleavage of **1**. No reaction occurs between **1** and ethene. Interestingly, $[NBu_4][W_2Cl_7(\eta\text{-}C_2Me_2)_2]$ **7** shows no reactivity towards C_2Me_2.

Treatment of a dichloromethane solution of **1** with pyridine (2–3 equivalents) gave a pale green-brown solution. Examination of the crude product by ^1H NMR spectroscopy showed a complex mixture of products with no evidence for the mononuclear species $[WCl_4(\eta\text{-}C_2Me_2)(py)]$ **3**. No single compound could be separated from the mixture and this reaction was not pursued. Similarly, treatment of solutions of **1** with MeCN or PPh_3 (2 equivalents) gave rise to pale green-brown solutions from which no tractable product could be separated. It may be of relevance that the dimolybdenum species $[Mo_2Cl_4(\mu\text{-}Cl)_2(\mu\text{-}C_2Bu^t_2)(OPCl_3)_2]$ undergoes dimer cleavage reactions with loss of $POCl_3$ and $C_2Bu^t_2$ even with weak donor ligands such as chloride ions.[12] It is also noted that no reaction chemistry of $[Ta_2Cl_4(\mu\text{-}Cl)_2(\mu\text{-}C_2Bu^t_2)(thf)_2]$ has been reported, although Cotton and co-workers[17,25] have recently begun to develop a rather extensive alkyne chemistry with niobium supported by chloride ligands.

In contrast to its reactions with the neutral donor ligands, **1** undergoes sequential thf exchange with one or two equivalents of $[N(PPh_3)_2]Cl$ to give the compounds $[N(PPh_3)_2][W_2Cl_5(\mu\text{-}Cl)_2(\mu\text{-}C_2Me_2)(thf)]$ **8** and $[N(PPh_3)_2]_2[W_2Cl_6(\mu\text{-}Cl)_2(\mu\text{-}C_2Me_2)]$ **9** respectively in quantitative yields. The identities of **8** and **9** were elucidated by elemental analysis, and ^1H and ^{13}C NMR spectroscopy. Thus **8** shows resonances assignable to one $[N(PPh_3)_2]^+$ cation and to one co-ordinated C_2Me_2 and thf ligand, whereas **9** has resonances assignable to two $[N(PPh_3)_2]^+$ cations and one μ-C_2Me_2 ligand with no co-ordinated thf. Both **8** and **9** show ^{183}W satellites in their ^{13}C NMR spectra with relative area 26–29%, consistent with the maintenance of a dimetallatetrahedrane moiety. Compound **8** may also be prepared from an equimolar mixture of **1** and **9** *via* a ligand redistribution reaction.

For the three but-2-yne derivatives **1**, **8** and **9** there is an apparent correlation between increasing negative charge on the complex and a shift to higher field of the C_{ac} resonance (δ 234.8, 223.9 and 220.2 ppm respectively), consistent with increased shielding of the C_{ac} nucleus with build-up of negative charge.

Suppression of a Second-order Jahn–Teller Distortion in the New Perpendicular Bridge Alkyne Complexes.—To probe further the metal–alkyne bonding in the $[W_2Cl_4(\mu\text{-}Cl)_2(\mu\text{-}RC_2R')(thf)_2]$ complexes, extended Hückel molecular orbital calculations[26] were carried out. The atomic parameters used in the calculations were taken from previous work.[27] A general

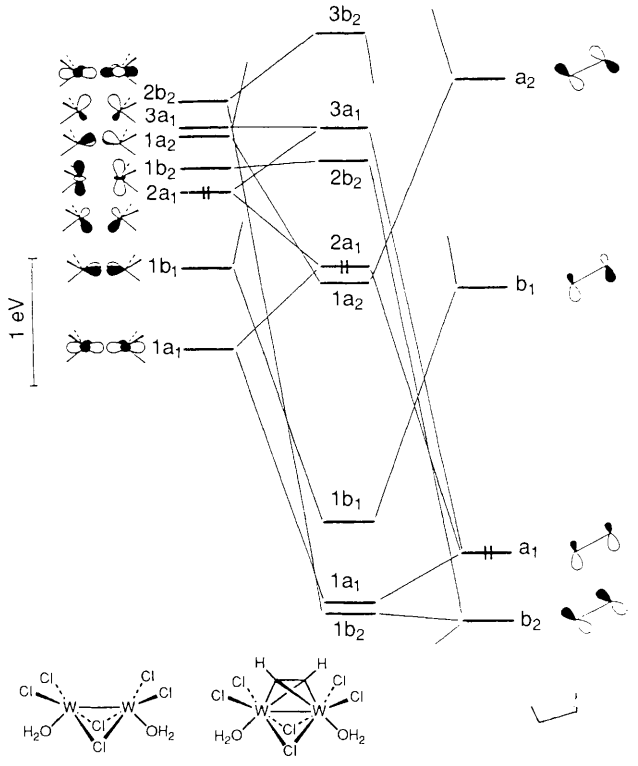

Fig. 4 Interaction diagram for $[W_2Cl_4(\mu\text{-}Cl)_2(\mu\text{-}C_2H_2)(OH_2)_2]$ with symmetry labels appropriate to the C_{2v} point group

description of the bonding in parallel and perpendicular bridge alkyne compounds has been reported by Hoffmann and co-workers.[21] More recently, Chisholm *et al.*[23] have published Fenske–Hall molecular orbital calculations for the various geometries of alkoxide-supported perpendicular bridge alkyne complexes,[23] and Cotton and Feng[28] have carried out Xα-SW calculations on the halide-supported niobium and tantalum systems, in addition to the amido-bridged tungsten system previously analysed by Calhorda and Hoffmann.[14]

The molecular orbital study undertaken employed the model complex $[W_2Cl_4(\mu\text{-}Cl)_2(\mu\text{-}C_2H_2)(OH_2)_2]$ with an initial geometry based on the crystal structure of **4** and idealised to C_{2v} symmetry, with thf replaced by H_2O. The fragment analysis approach has proved to be a straightforward way of understanding the interaction of an alkyne fragment with a metal centre and the results of an extended Hückel calculation on $[W_2Cl_4(\mu\text{-}Cl)_2(\mu\text{-}C_2H_2)(OH_2)_2]$ are shown in the form of a molecular orbital interaction diagram in Fig. 4. The fragment orbitals of *cis* bent C_2H_2 are depicted in Fig. 4, and an account of their shapes and relative energies have been given previously.[21,23] The frontier orbitals of the dimetal fragment $W_2Cl_4(\mu\text{-}Cl)_2(OH_2)_2$ are similar to the frontier orbitals of the related fragments $[W_2Cl_6(\mu\text{-}NH_2)_2]^{2-}$, $[W_2(OH)_4(\mu\text{-}OH)_2(NH_3)_2]$[23] and $[M_2Cl_4(\mu\text{-}Cl)_2H_2]^{2-}$ (M = Mo or Ta)[21] whose derivation has been given elsewhere.

The result of allowing *cis* bent C_2H_2 to interact with the metal fragment to produce $[W_2Cl_4(\mu\text{-}Cl)_2(\mu\text{-}C_2H_2)(OH_2)_2]$ is shown in the centre of Fig. 4. The five highest occupied molecular orbitals of the resultant complex accommodate the 10 electrons from the frontier orbitals of the dimetal and alkyne fragments. The $1a_1$ and $1b_2$ orbitals are ligand-based and predominantly alkyne in character while the $1b_1$, $1a_2$ and $2a_1$ orbitals are essentially metal-based. The $2a_1$ orbital is the metal-based, antibonding counterpart to the metal-ligand bonding $1a_1$ orbital at lower energy. The $2a_1$ orbital is predominantly metal–metal bonding in character and represents a metal–metal σ bond in this complex. By contrast, the $1b_2$ and $1a_2$ orbitals contain much more equal metal and ligand combinations. These orbitals are strongly metal–ligand bonding and represent π-back-bonding from metal d to alkyne π* orbitals. Detailed discussions of these interactions and Mulliken population analyses have been given elsewhere.[21,23]

The $2a_1$ and $1a_2$ levels are very close in energy and we have found their ordering to be very senstitive to the degree of interaction allowed between the dimetal and alkyne fragments. A slightly different level ordering of the metal-based orbitals ($1b_1 < 2a_1 < 1a_2$) was computed for the model complexes $[M_2Cl_4(\mu\text{-}Cl)_2(\mu\text{-}C_2H_2)H_2]^{2-}$ (M = Mo or Ta) but otherwise the principal results of our calculations appear to be very similar to those described earlier for these related systems.[21]

Bridging alkyne compounds have been classified according to idealised parallel (θ = 90°) or perpendicular (θ = 0°) bridge geometries. Small deviations from these two extremes have been observed in the past but have usually been attributed to steric factors or crystal-packing forces. Two recent reports,[5,29] however, have demonstrated the validity of earlier predictions concerning possible second-order Jahn–Teller distortions in some perpendicular bridge complexes.[21,30]

Of particular relevance to us here is the ditungsten system $[W_2Cl_4(\mu\text{-}NMe_2)_2(\mu\text{-}C_2Me_2)(py)_2]$ in which the bridging C_2Me_2 ligand shows a marked deviation from the idealised perpendicular bridge geometry being twisted by 35° from the ideal (θ = 0°) perpendicular bridge geometry.[5] This distortion was investigated by Calhorda and Hoffmann[14] using extended Hückel computational procedures and was attributed to a second-order Jahn-Teller distortion.[31] More recently, Cotton and Feng[28] have examined similar distortions in a series of Nb, Mo, Ta and W complexes using the Xα-SW method. They concluded that the presence or absence of a Jahn-Teller distortion is a general key to understanding the structures.

Hoffmann's calculations for the model complex $[W_2Cl_6(\mu\text{-}NH_2)_2(\mu\text{-}C_2H_2)]^{2-}$ {with a geometry based on the crystal structure of $[W_2Cl_4(\mu\text{-}NMe_2)_2(\mu\text{-}C_2Me_2)(py)_2]$} found a very small highest occupied molecular orbital (HOMO)–lowest unoccupied molecular orbital (LUMO) gap indicative of an incipient second-order Jahn–Teller distortion.[14] The alkyne twisting is of A_2 symmetry and allows the HOMO (a_1 symmetry) and LUMO (a_2) to mix ($a_2 \times a_1 = A_2$) thus stabilising the system. The calculated total energy curve for rotation of the $\mu\text{-}C_2H_2$ fragment above the $[W_2Cl_6(\mu\text{-}NH_2)_2]^{2-}$ moiety showed a shallow minimum for a rotation of θ = 26° for this hypothetical hexachloride environment.

The alkyne rotation is inhibited by destabilisation of the $1a_1$ orbital which is W–C bonding and W–Cl antibonding. As rotation proceeds, an antibonding interaction develops and the orbital rises in energy. The twist observed in $[W_2Cl_4(\mu\text{-}NMe_2)_2(\mu\text{-}C_2Me_2)(py)_2]$ was investigated by considering the model complex $[W_2Cl_4(\mu\text{-}NH_2)_2(\mu\text{-}C_2H_2)H_2]^{2-}$ which gave a similar interaction diagram to that of $[W_2Cl_6(\mu\text{-}NH_2)_2(\mu\text{-}C_2H_2)]^{2-}$. However, the calculations now predicted a much deeper total energy minimum at a larger rotation (θ *ca.* 40°) because there is no hydrogen participation in the $1a_1$ orbital of this complex.

The $\mu\text{-}C_2Me_2$ ligand in $[W_2Cl_4(\mu\text{-}Cl)_2(\mu\text{-}C_2Me_2)(thf)_2]$ **1** shows a small twist (θ *ca.* 9°) from the ideal perpendicular bridge geometry (Fig. 1), whereas for the less sterically demanding $\mu\text{-}C_2H_2$ ligand in $[W_2Cl_4(\mu\text{-}Cl)_2(\mu\text{-}C_2H_2)(thf)_2]$ **4** only a negligible distortion (θ < 5°) was observed (Fig. 3). Furthermore, the interaction diagram for $[W_2Cl_4(\mu\text{-}Cl)_2(\mu\text{-}C_2H_2)(OH_2)_2]$ (Fig. 4), based on the experimentally observed geometry of **4**, shows a substantial HOMO–LUMO gap, and an even larger energy separation between $3a_1$ and $1a_2$. Rotation of the alkyne above the W_2 fragment in this complex showed that the minimum in the total energy curve was located at, or very close to, θ = 0°, *A priori*, a significant second-order Jahn–Teller distortion would not be expected for the complexes $[W_2Cl_4(\mu\text{-}Cl)_2(\mu\text{-}RC_2R')(thf)_2]$.

The differences between the computational results described here and those reported by Hoffmann for $[W_2Cl_6(\mu\text{-}NH_2)_2$-

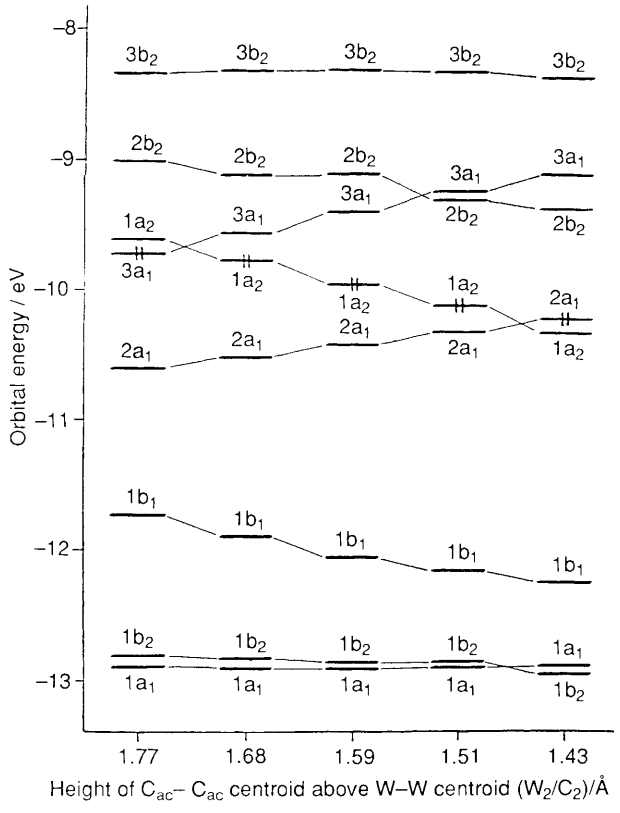

Fig. 5 Changes in level ordering on increasing the degree of metal–alkyne interaction in $[W_2Cl_4(\mu\text{-}Cl)_2(\mu\text{-}C_2H_2)(OH_2)_2]$

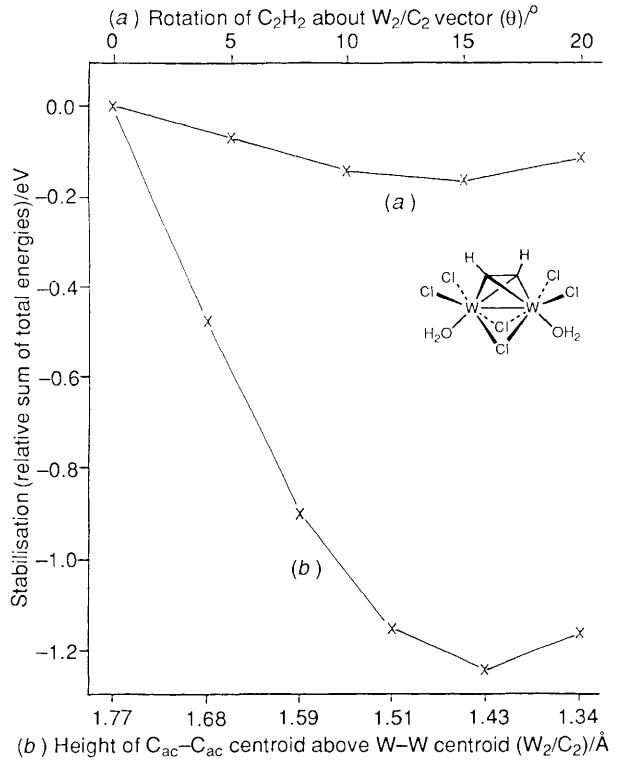

Fig. 6 (*a*) Total energy curve for rotation of the alkyne in the weakly bound alkyne complex $[W_2Cl_4(\mu\text{-}Cl)_2(\mu\text{-}C_2H_2)(OH_2)_2]$. (*b*) Total energy curve for increasing the metal–alkyne interaction from a weakly bound to a strongly bound alkyne complex $[W_2Cl_4(\mu\text{-}Cl)_2(\mu\text{-}C_2H_2)(OH_2)_2]$

$(\mu\text{-}C_2H_2)]^{2-}$ may be traced to the extent of metal–alkyne interaction assumed in the two models. In Hoffmann's calculations,[14] shorter W–W and C_{ac}–C_{ac} bond lengths were assumed, and the alkyne was allowed to rotate at a larger height above the W–W bond. We shall refer to this as a 'weakly bound' alkyne complex. The $[W_2Cl_4(\mu\text{-}Cl)_2(\mu\text{-}C_2R_2)(thf)_2]$ complexes reported here have substantially longer W–W and C_{ac}–C_{ac} bonds, and may be referred to as 'strongly bound' alkyne complexes. We repeated our calculations for $[W_2Cl_4(\mu\text{-}Cl)_2(\mu\text{-}C_2H_2)(OH_2)_2]$, but this time assuming initial values of 2.436, 1.376 and 1.77 Å {taken from the crystal structure of $[W_2Cl_4(\mu\text{-}NMe_2)_2(\mu\text{-}C_2Me_2)(py)_2]$[5]} for W–W, C_{ac}–C_{ac} and W_2/C_2 (where W_2/C_2 is the height of the C_{ac}–C_{ac} centroid above the W–W bond centroid). The level ordering for this weakly bound alkyne complex is shown on the left in Fig. 5.

The relationship between the weakly- and strongly-bound alkyne complexes can be found by monitoring the changes in level ordering as the metal–alkyne interaction is allowed to develop from the one extreme to the other. The results are shown in Fig. 5 in the form of a Walsh diagram in which linear relationships between W–W, C_{ac}–C_{ac} and W_2/C_2 were assumed. The level ordering at the far left of Fig. 5 (for the weakly bound alkyne complex) closely resembles that obtained previously for $[W_2Cl_6(\mu\text{-}NH_2)_2(\mu\text{-}C_2H_2)]^{2-}$, and the small HOMO–LUMO gap suggests a possible second-order Jahn–Teller distortion. Note the consequences of changing the extent of metal–alkyne interaction. The $1a_2$ orbital is now a low-lying LUMO; in other words the alkyne is much less reduced since one alkyne π^* orbital ($1a_2$ in Fig. 4) is effectively unoccupied, and the metal–metal bonding is much stronger. When the alkyne was allowed to rotate above the W–W vector, a small and shallow minimum at θ *ca.* 15° was found in the total energy curve. A principal feature of Fig. 5 is the driving apart of the $3a_1$ and $1a_2$ levels as the metal–alkyne interaction develops. The stabilisation of $1a_2$ is one of the key factors in this process and represents enhanced metal–alkyne back-bonding. The other orbital which is dominant in stabilising a more strongly bound alkyne is $1b_1$ which is also involved in metal–alkyne back-donation.

These results suggest that a complex of the type $[W_2Cl_4(\mu\text{-}Cl)_2(\mu\text{-}C_2H_2)(OH_2)_2]$ with a *weak* metal–alkyne interaction (far left in Fig. 5) *would* be expected to undergo a second-order Jahn–Teller distortion, while a similar complex with a *strong* metal–alkyne interaction (far right in Fig. 5) is *unlikely* to do so. Fig. 6 shows a comparison of the total energy curves for (*a*) the alkyne rotation in the weakly bound alkyne complex and (*b*) for the conversion of the weakly bound alkyne complex to the strongly bound alkyne complex. In the latter curve an extrapolation has been made to a complex containing an alkyne more tightly bound than for **4** in order to locate the minimum in this curve.

The large difference between the computed minima of the total energy curves for the two possibilities strongly favours increased metal–alkyne bonding over the alternative second-order Jahn–Teller distortion. A particular feature of the lower curve is a minimum in the region of the solid-state geometry found for **4**. In general, total energy curves obtained from extended Hückel techniques need to be treated with caution. However, the large computed total energy difference for the two alternative processes, together with the location of an energy minimum in the expected region of curve (*b*), lends support to the validity of these results.

We were interested to see if total energy curves for $[W_2Cl_4(\mu\text{-}Cl)_2(\mu\text{-}C_2H_2)H_2]^{2-}$ would favour a second-order Jahn-Teller distortion over the alternative strong alkyne bonding. Fig. 7 shows a comparison of the total energy curves for (*a*) the rotation of the alkyne in a weakly bound alkyne complex and (*b*) for the conversion of a weakly bound alkyne complex to a strongly bound alkyne complex. In this case the larger stabilisation afforded by the second-order Jahn–Teller distortion wins out over the alternative increase in metal–alkyne bonding, a result consistent with the substantially twisted geometry observed for $[W_2Cl_4(\mu\text{-}NMe_2)_2(\mu\text{-}C_2Me_2)(py)_2]$.[5]

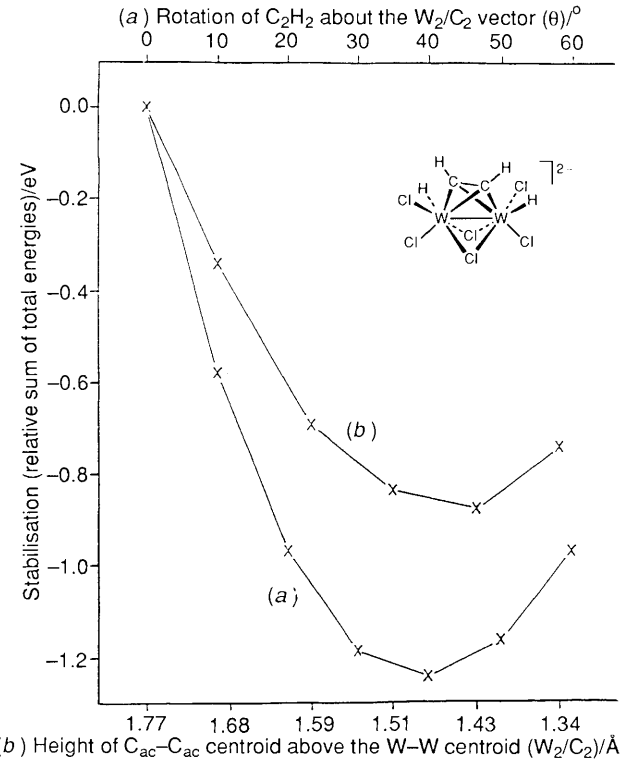

Fig. 7 (*a*) Total energy curve for rotation of the alkyne in the weakly bound alkyne complex $[W_2Cl_4(\mu\text{-}Cl)_2(\mu\text{-}C_2H_2)H_2]^{2-}$. The sense of rotation of C_2H_2 is towards the hydride ligand. (*b*) Total energy curve for increasing the metal–alkyne interaction from a weakly to a strongly bound alkyne complex $[W_2Cl_4(\mu\text{-}Cl)_2(\mu\text{-}C_2H_2)H_2]^{2-}$

Experimental

All manipulations of air- and moisture-sensitive materials were performed using either standard Schlenk-line techniques under an atmosphere of dinitrogen, which had been purified by passage over BASF catalyst and 4 Å molecular sieves, or in an intert-atmosphere dry box containing dinitrogen. Solvents were pre-dried by standing over 4 Å molecular sieves and then distilled under an atmosphere of dinitrogen from phosphorus pentaoxide (dichloromethane), sodium (toluene), sodium–potassium alloy (diethyl ether; light petroleum, b.p. 40–60 °C) or potassium–benzophenone (thf). $[^2H_2]$Dichloromethane for NMR studies was dried over phosphorus pentaoxide and stored in a Youngs ampoule under an atmosphere of dinitrogen. Celite 545 Filter Aid was used as supplied by Koch-Light Laboratories Ltd.

Pyridine, $[N(PPh_3)_2]Cl$, $[NBu_4]Cl$, C_2Me_2, HC_2Ph and C_2Et_2 were used as received (Aldrich), C_2H_2 was passed through a cold trap at −78 °C prior to use, and WCl_4 and $Na[W_2Cl_7(thf)_5]$ were prepared as described previously.[10]

Elemental analyses were performed by the analytical department of this laboratory. Proton and ^{13}C NMR spectra were recorded either on a Brüker WH 300 (^1H, 300 MHz), a Brüker AM 250 (^{13}C, 62.9 MHz) or a Brüker AM 300 (^1H, 300 MHz; ^{13}C, 75.5 MHz) spectrometer. Carbon-13 spectra were recorded using a gated sequence to give nuclear Overhauser effect enhancement. Spectra were referenced internally using the residual protio solvent (^1H) and solvent (^{13}C) resonances relative to tetramethylsilane (δ 0 ppm) with chemical shifts quoted in δ (ppm) and coupling constants in Hz. Infrared spectra were recorded as Nujol mulls on CsI plates using a Perkin-Elmer 1510 FT Interferometer.

The molecular orbital calculations were performed using a modified extended Hückel method employing weighted H_{ij} values.[26] The atomic coordinates were idealised to C_{2h} symmetry, but otherwise initial bond lengths (*i.e.*, for the strongly bound alkyne complex) [W–W 2.624, W–C_{ac} 2.065, C_{ac}–C_{ac} 1.41, C–H 1.05, O–H 1.00, W–Cl(terminal) 2.344, W–Cl(bridge) 2.486 and W–O 2.22 Å] and angles [W–W–Cl(terminal) 126.0, O–W–Cl(terminal) 82.7, W–W–Cl(bridge) 58.1, W–W–O 128.0, Cl(terminal)–W–Cl(terminal) 93.8, Cl(terminal)–W–Cl(bridge) 92.6, Cl(bridge)–W–Cl(bridge) 78.1, C_{ac}–C_{ac}–H 134.5 and H–O–H 120.0°] were taken from the crystal structure of $[W_2Cl_4(\mu\text{-}Cl)_2(\mu\text{-}C_2H_2)(thf)_2]$ **4**. The atomic parameters were taken from previous work.[27]

Preparation of $[W_2Cl_4(\mu\text{-}Cl)_2(\mu\text{-}C_2Me_2)(thf)_2]$ **1**.—A solution of $Na[W_2Cl_7(thf)_5]$ (2 g, 2.01 mmol) and but-2-yne (0.75 g, 13.9 mmol) in thf (200 cm^3) was stirred at room temperature (r.t.) for 18 h giving a green-brown solution and a grey precipitate. The volatiles were removed under reduced pressure and the residues extracted with toluene–dichloromethane (3:1 v/v, 2 × 200 cm^3), filtered through a bed of Celite and the volatiles removed under reduced pressure. The solid was extracted with dichloromethane and filtered through a short column of Celite. Removal of volatiles under reduced pressure afforded crude green **1** (600 mg, 40%) which could be used in further reactivity studies without additional purification. Analytically pure **1** may be obtained by recrystallisation from a minimum volume of dichloromethane at −80 °C.

Preparation of $[WCl_4(\eta\text{-}C_2Me_2)(thf)]$ **2**.—*Method* 1. Treatment of crude **1** (600 mg) in dichloromethane (20 cm^3) with an excess of but-2-yne (*ca.* 1 g) gave a red-brown solution which was reduced in volume and cooled to *ca.* −80 °C. Green microcrystals of **2** were washed with cold dichloromethane (2 × 5 cm^3) and light petroleum (3 × 10 cm^3) and dried *in vacuo*. Yield, 11%.

Method 2. A suspension of WCl_4 (2.6 g, 8 mmol) in diethyl ether (60 cm^3) was treated with but-2-yne (0.9 g, 16 mmol). After 14 d, the green solution was filtered (to remove unreacted WCl_4), the volatiles removed under reduced pressure and the green residues dissolved in thf (40 cm^3). After 20 h the thf was removed under reduced pressure to give green, spectroscopically pure **2**. Yield, 2.05 g (60%).

Preparation of $[WCl_4(\eta\text{-}C_2Me_2)(py)]$ **3**.—A solution of $[WCl_4(\eta\text{-}C_2Me_2)(thf)]$ **1** (0.28 g, 0.55 mmol) in dichloromethane (30 cm^3) was treated with pyridine (*ca.* 2 cm^3) to afford a green-brown solution. After 8 h, the volatiles were removed under reduced pressure to give spectroscopically pure **3**. Yield, *ca.* 100%. Analytically pure **3** may be obtained by crystallisation from thf–toluene at −25 °C.

Preparation of $[W_2Cl_4(\mu\text{-}Cl)_2(\mu\text{-}C_2H_2)(thf)_2]$ **4**.—Ethyne (5 mmol) was condensed onto a frozen solution of $Na[W_2Cl_7(thf)_5]$ (1 g, 1.01 mmol) in thf (160 cm^3) and the matrix warmed carefully to room temperature. After 9 h the volatiles were removed under reduced pressure and the red-brown residues extracted with toluene (3 × 20 cm^3) and then dichloromethane (4 × 15 cm^3). The dichloromethane extracts were reduced to *ca.* 15 cm^3 and cooled to −80 °C affording green microcrystalline **4**. Yield, 200 mg (30%).

Preparation of $[W_2Cl_4(\mu\text{-}Cl)_2(\mu\text{-}C_2Et_2)(thf)_2]$ **5**.—Hex-3-yne (0.55 g, 6.7 mmol) and $Na[W_2Cl_7(thf)_5]$ (1.1 g, 1.1 mmol) were dissolved in thf (120 cm^3). After 3 d a grey precipitate had formed and the supernatant was emerald green. Volatiles were removed under reduced pressure and the green-brown residues were extracted with toluene (4 × 20 cm^3). After filtration and reducing the volume to 15 cm^3, cooling to −80 °C gave green microcrystals of **5**. Yield, 210 mg (25%).

Preparation of $[W_2Cl_4(\mu\text{-}Cl)_2(\mu\text{-}HC_2Ph)(thf)_2]$ **6**.—Phenylethyne (0.56 g, 5.5 mmol) and $Na[W_2Cl_7(thf)_5]$ (1 g, 1.01 mmol) were dissolved in thf (100 cm^3). After 7 h, the volume was reduced to *ca.* 10 cm^3 and light petroleum (50 cm^3) was added giving a light brown solid which was then washed thoroughly

Table 8 Crystallographic data for **1**, **2** and **4**

Complex	**1**	**2**	**4**
Formula	$C_{12}H_{22}Cl_6O_2W_2$	$C_8H_{14}Cl_4OW$	$C_{10}H_{18}Cl_6O_2W_2$
M	778.72	451.86	750.66
Crystal size/mm	0.10 × 0.25 × 0.45	0.30 × 0.40 × 0.40	0.10 × 0.35 × 0.05
Colour	Green	Green	Green
Crystal system	Monoclinic	Monoclinic	Monoclinic
Space group	$P2/c$	$P2_1/c$	$C2/c$
a/Å	10.028(3)	7.782(1)	21.676(6)
b/Å	7.894(3)	7.167(2)	7.144(2)
c/Å	13.298(2)	23.741(5)	12.637(3)
β/°	105.96(2)	95.67(1)	111.48(2)
U/Å^3	1012.1	1317.6	1824(3)
Z	2	4	4
D_c/g cm^{-3}	2.56	2.28	2.74
μ/cm^{-1}	124.10	97.44	137.70
F(000)	720	848	1376
Radiation (λ/Å)	Mo-Kα (0.710 69)	Mo-Kα (0.710 69)	Mo-Kα (0.710 69)
2θ limits/°	2–50	3–50	3–50
Scan mode	ω–2θ	ω–2θ	ω–2θ
Scan angle/°	0.90 + 0.35 (tan θ)	0.90 + 0.35 (tan θ)	0.85 + 0.35 (tan θ)
Horizontal aperture/mm	4.0	3.0	2.5
Zone	$h, k, \pm l$	$h, k, \pm l$	$h, k, \pm l$
Total data collected	2036	2996	2694
No. of observations [$I > 3\sigma(I)$]	1386	1961	1005
No. of variables	100	130	92
Obs./variables	13.9	15.1	10.9
Weighting scheme	Chebyshev	Chebyshev	Chebyshev
Weighting coefficients	6.302, −3.238, 4.313	9.089, −6.350, 6.816	7.333, 0.914, 6.724
R(merg)	0.029	0.027	0.045
R^a	0.031	0.029	0.059
R'^b	0.037	0.034	0.066

^{a} $R = \Sigma(|F_o| - |F_c|)/(\Sigma|F_o|)$. ^{b} $R' = \sqrt{[\Sigma w(|F_o| - |F_c|)^2/\Sigma w|F_o|^2]}$.

with light petroleum. Subsequent extraction with toluene (3 × 40 cm^3), filtration, reduction of volume to *ca.* 35 cm^3 and cooling to −80 °C afforded light green microcrystals of **6**. Elemental analysis of this product indicated varying amounts of toluene which could not be removed *in vacuo*. Dissolution of the product in dichloromethane (40 cm^3) and subsequent removal of volatiles under reduced pressure gave **6** as a green solid, which analysed for one mole of dichloromethane per mole of **6**. Yield, 300 mg (35%).

Reactions of $Na[W_2Cl_7(thf)_5]$ *with* C_2R_2 (R = Ph, CF_3 *or* $SiMe_3$).—*With* C_2Ph_2. A solution of diphenylethyne (0.8 g, 4.5 mmol) and $Na[W_2Cl_7(thf)_5]$ (0.88 g, 8.8 mmol) in thf (100 cm^3) was heated under reduced pressure at 45 °C for 3 d. Examination of the red-brown solution by ^{1}H NMR spectroscopy showed no evidence for a η- or μ-bound C_2Ph_2 ligand.

With $C_2(CF_3)_2$ *or* $C_2(SiMe_3)_2$. A solution of the alkyne (5 mmol) and $Na[W_2Cl_7(thf)_5]$ (1 g, 1.01 mmol) in thf (100 cm^3) was heated under reduced pressure in a Youngs ampoule for 6 d. No reaction occurred and $Na[W_2Cl_7(thf)_5]$ was recovered.

Preparation of $[NBu^n_4][W_2Cl_4(\mu\text{-}Cl)_3(\eta\text{-}C_2Me_2)_2]$ **7**.—To a solution of $Na[W_2Cl_7(thf)_5]$ (0.5 g, 0.5 mmol) in dichloromethane (50 cm^3) was added $[NBu^n_4]Cl$ (0.14 g, 0.5 mmol). After 16 h, the solution was filtered through Celite and but-2-yne (0.12 g, 2.3 mmol) in dichloromethane (10 cm^3) was added, giving a red-brown solution after 3 h. Layering of the solution with toluene afforded maroon microcrystals of **7** which were washed with cold dichloromethane (2 × 5 cm^3) and dried *in vacuo*. Yield, 110 mg (27%).

Preparation of $[N(PPh_3)_2][W_2Cl_5(\mu\text{-}Cl)_2(\mu\text{-}C_2Me_2)(thf)]$ **8**.—A solution of $[W_2Cl_4(\mu\text{-}Cl)_2(\mu\text{-}C_2Me_2)(thf)_2]$ (0.225 g, 0.29 mmol) in dichloromethane (15 cm^3) was treated with $[N(PPh_3)_2]Cl$ (0.17 g, 0.29 mmol) in dichloromethane (10 cm^3) giving a turquoise solution. After 3 h, the volatiles were removed under reduced pressure to afford **8** as an analytically pure microcrystalline turquoise solid. Yield *ca.* 100%.

Preparation of $[N(PPh_3)_2]_2[W_2Cl_6(\mu\text{-}Cl)_2(\mu\text{-}C_2Me_2)]$ **9**.—A solution of $[W_2Cl_4(\mu\text{-}Cl)_2(\mu\text{-}C_2Me_2)(thf)_2]$ (90 mg, 0.12 mmol) in dichloromethane (15 cm^3) was treated with $[N(PPh_3)_2]Cl$ (133 mg, 0.24 mmol) in dichloromethane (10 cm^3). After 3 h, the volatiles were removed under reduced pressure to afford analytically pure **9** as a turquoise microcrystalline solid. Yield, *ca.* 100%.

X-Ray Crystal-structure Determinations of **1**, **2** *and* **4**.—Crystal data and collection and processing parameters are given in Table 8. The general procedure was as follows. A crystal was sealed in a Lindemann glass capilliary and transferred to the goniometer head of an Enraf-Nonius CAD4-F diffractometer interfaced to a PDP 11/23 and LSI minicomputer. Unit-cell parameters were calculated from the setting angles of 25 carefully centred reflections. Three reflections were chosen as intensity standards and were measured every 3600 s of X-ray exposure time, and three orientation controls were measured every 250 reflections.

The data were corrected for Lorentz and polarisation effects and an empirical absorption correction[32] based on an azimuthal scan was applied. Equivalent reflections were merged and systematically absent reflections rejected. The tungsten atom position was determined from a Patterson synthesis. Subsequent difference Fourier syntheses revealed the positions of other non-hydrogen atoms. Non-hydrogen atoms were refined with anisotropic thermal parameters by least-squares procedures. Hydrogen atoms were placed in estimated positions and refined riding on their supporting carbon atoms. A Chebyshev weighting scheme[33] was applied and the data were corrected for the effects of anomalous dispersion and isotropic extinction (*via* an overall isotropic extinction parameter[34]) in the final stages of refinement. For complexes **1** and **4** where

examination of the systematic extinctions do not uniquely define the space group, we examined the possibility of refinement in the corresponding non-centrosymmetric space groups (*Pc* and *Cc* respectively) but found the refinement less satisfactory. These results are consistent with the analysis of the Wilson statistics for the reflection data.

All crystallographic calculations were performed using the CRYSTALS suite[35] on a VAX 11/750 computer in the Chemical Crystallography Laboratory, Oxford. Scattering factors were taken from the usual sources.[36]

Additional material available from the Cambridge Crystallographic Data Centre comprises H-atom coordinates, thermal parameters and remaining bond lengths and angles.

Acknowledgements

We thank the SERC and BP plc for a CASE award (to P. M.).

References

1 M. H. Chishom, *Polyhedron*, 1988, **7**, 757.
2 M. J. Winter, *Adv. Organomet. Chem.*, 1989, **29**, 101.
3 R. S. Dickson and P. J. Fraser, *Adv. Organomet. Chem.*, 1974, **12**, 323.
4 W. A. Buhro and M. H. Chisholm, *Adv. Organomet. Chem.*, 1987, **27**, 311.
5 K. J. Ahmed, M. H. Chisholm, K. Folting and J. C. Huffman, *Organometallics*, 1986, **5**, 2171.
6 F. A. Cotton and W. T. Hall, *Inorg. Chem.*, 1980, **19**, 2354.
7 F. A. Cotton and W. T. Hall, *J. Am. Chem. Soc.*, 1979, **101**, 5094.
8 F. A. Cotton and W. T. Hall, *Inorg. Chem.*, 1981, **20**, 1285.
9 F. A. Cotton and W. T. Hall, *Inorg. Chem.*, 1980, **19**, 2352.
10 M. H. Chisholm, B. W. Eichorn, K. Folting, J. C. Huffman, C. D. Ontiveros, W. E. Streib and W. G. Van Der Sluys, *Inorg. Chem.*, 1987, **26**, 3182.
11 S. G. Bott, D. L. Clark, M. L. H. Green and P. Mountford, *J. Chem. Soc., Chem. Commun.*, 1989, 418.
12 E. Hey, F. Weller, B. Simon, G. Becker and K. Dehnicke, *Z. Anorg. Allg. Chem.*, 1983, **501**, 61.
13 K. J. Ahmed, M. H. Chisholm, K. Folting and J. C. Huffman, *J. Chem. Soc., Chem. Commun.*, 1985, 152.
14 M. J. Calhorda and R. Hoffmann, *Organometallics*, 1986, **5**, 2181.
15 K. H. Theopold, S. J. Holmes and R. R. Schrock, *Angew. Chem. Suppl.*, 1983, 1409.
16 E. Hey, F. Weller and K. Dehnicke, *Z. Anorg. Allg. Chem.*, 1984, **514**, 18; M. Kersting, K. Dehnicke and D. Fenske, *J. Organomet. Chem.*, 1988, **346**, 201; V. G. Uhl, E. Hey, G. Becker, F. Weller and K. Dehnicke, *Z. Anorg. Allg. Chem.*, 1983, **497**, 213.
17 F. A. Cotton and M. Shang, *Inorg. Chem.*, 1990, **29**, 508.
18 J. L. Templeton and B. C. Ward, *J. Am. Chem. Soc.*, 1980, **102**, 3288.
19 D. S. Ginley, C. R. Bock, M. S. Wrighton, B. Fischer, D. T. Tipton and R. Bau, *J. Organomet. Chem.*, 1978, **157**, 41; M. H. Chisholm, K. Folting, J. C. Huffman and I. P. Rothwell, *J. Am. Chem. Soc.*, 1982, **104**, 4389.
20 R. E. McCarley and J. L. Templeton, *Inorg. Chem.*, 1978, **17**, 1263.
21 D. M. Hoffman, R. Hoffmann and C. R. Fisel, *J. Am Chem. Soc.*, 1982, **104**, 3858.
22 F. A. Cotton, J. D. Jamerson and B. R. Stults, *J. Am. Chem. Soc.*, 1976, **98**, 1774.
23 M. H. Chisholm, B. K. Conroy, D. L. Clark and J. C. Huffman, *Polyhedron*, 1988, **7**, 903.
24 D. J. Bergs, M. H. Chisholm, K. Folting, J. C. Huffman and K. A. Stahl, *Inorg. Chem.*, 1988, **27**, 2950.
25 F. A. Cotton and M. Shang, *J. Am. Chem. Soc.*, 1990, **112**, 1584.
26 R. Hoffmann and W. N. Lipscomb, *J. Chem. Phys.*, 1962, **36**, 2179.
27 R. Hoffmann, *J. Chem. Phys.*, 1963, **39**, 1397; R. H. Summerville and R. Hoffmann, *J. Am. Chem. Soc.*, 1976, **98**, 7240; A. Dedieu, T. A. Albright and R. Hoffmann, *J. Am. Chem. Soc.*, 1979, **101**, 3141.
28 F. A. Cotton and X. Feng, *Inorg. Chem.*, 1990, **29**, 3197.
29 R. P. Aggarwal, N. G. Connelly, M. C. Crespo, B. J. Dunne, P. M. Hopkins and A. G. Orpen, *J. Chem. Soc., Chem. Commun.*, 1989, 33.
30 D. L. Thorn and R. Hoffmann, *Inorg. Chem.*, 1978, **17**, 126.
31 For a discussion see, T. A. Albright, J. K. Burdett and M.-H. Whangbo, *Orbital Interactions in Chemistry*, Wiley-Interscience, New York, 1985, p. 95.
32 A. C. T. North, D. C. Philips and F. S. Mathews, *Acta Crystallogr., Sect. A*, 1968, **24**, 351.
33 J. S. Rollet, *Computing Methods in Crystallography*, Pergamon Press, Oxford, 1965.
34 A. C. Larson, *Acta Crystallogr., Sect. A*, 1967, **23**, 664.
35 D. J. Watkin, J. R. Carruthers and P. W. Betteridge, CRYSTALS User Guide, Chemical Crystallography Laboratory, University of Oxford, 1985.
36 *International Tables for X-Ray Crystallography*, Kynoch Press, Birmingham, 1974, vol. 4.

Received 15*th August* 1990; *Paper* 0/03752D